Asian Herpetological Research 2015, 6(3): 189–198
DOI: 10.16373/j.cnki.ahr.140071

ORIGINAL ARTICLE

Comparative Studies on Sperm Ultrastructure of Three Gecko Species, *Gekko japonicus*, *Gekko chinensis* and *Hemidactylus bowrigii* (Reptilia, Squamata, Gekkonidae)

Shuangli HAO[1], Liangliang PAN[2], Zhouxi FANG[2] and Yongpu ZHANG[1*]

[1] *College of Life and Environmental Science, Wenzhou University, Wenzhou* 325035, *China*
[2] *College of Life Science, Wenzhou Medical University, Wenzhou* 325035, *China*

Abstract We provide the first description of the ultrastructure of the spermatozoa of *Gekko japonicus, Gekko chinensis* and *Hemidactylus bowrigii* for further understanding of the phylogenetic relationships of Gekkonidae. Mature spermatozoa of the three species differ in the occurrence and shape of epinuclear electron-lucent zone, nuclear space, neck cylinder and mitochondria. *G. japonicus* and *G. chinensis* have similar spermatozoan ultrastructure while *H. bowrigii* differs from these two species. In addition, these three species have neck cylinder with mitochondria in neck region and dense bodies arranged in grid with mitochondria in the midpiece, which may be the autapomorphies of the family Gekkonidae. Statistical analyses reveal that: total length of the spermatozoa was significantly different between *G. japonicus* and *G. chinensis*, as well as between *G. japonicus* and *H. bowrigii* ($F_{2,57} = 23.66$, $P < 0.0001$); *G. japonicus* and *H. bowrigii* differ in head length ($F_{2,43} = 4.64$, $P < 0.05$) and the width of nuclear base ($F_{2,22} = 3.97$, $P < 0.05$). In addition, the midpiece length ($F_{2,33} = 23.66$, $P < 0.01$) of the spermatozoa was significantly different between *H. bowrigii* and *G. japonicus*, and also between *H. bowrigii* and *G. chinensis*. Lengths of perforatorium, acrosomal complex and nuclear rostrum and the width of nuclear shoulder are similar in all three species. Our results indicated that the sperm ultrastructure contained intra and intergeneric variabilities which is helpful for better understanding their genetic relationships.

Keywords Spermatozoa, ultrastructure, Gekkonidae, phylogenetic relationship

1. Introduction

The sperm is a highly differentiated reproductive cell produced by testes and is a necessity in the fertilization process of Gekkonidae. Thus, any study on sperm ultrastructure is of great significance to help reveal the biological mechanisms of fertilization and reproductive biology. In addition, the ultrastructure of squamata sperm contains valuable phylogenetic information and provides important evidence for phylogenetic analyses (Jamiesion and Healy, 1992; Jamiesion, 1995; Oliver *et al.*, 1996; Teixeira *et al.*, 1999b, c; Vieira *et al.*, 2004; Vieira *et al.*, 2005; Zhang *et al.*, 2006). The sperm ultrastructure of squamata has rich polymorphism within the family (Giugliano *et al.*, 2002; Jamieson, 1995; Liu and Zhang, 2004; Oliver *et al.*, 1996; Teixeira *et al.*, 1999b, c; Tavares-Bastos *et al.*, 2002). Knowledge of the sperm ultrastructure improves the accuracy of the phylogenetic analysis, and contributes to the phylogenetic reconstruction in the higher order of classification (Giugliano *et al.*, 2002; Liu and Zhang, 2004; Tavares-Bastos *et al.*, 2002).

The Gekkonidae is widely distributed around the world and contains more than 90 genera and over 1000 named species (Han *et al.*, 2004). Other than Scincidae, it is the second-most-numerous family in sauria. However, detailed information on the ultrastructure of spermatozoa or spermiogenesis and studies clarifying the phylogenetic relationships of Gekkonidae remain obscure. Furieri (1970) briefly described the sperm

* Corresponding author: Prof. Yongpu ZHANG, Wenzhou University, Wenzhou, China, with his research focusing on physiological ecology and reproductive evolution of reptiles.
E-mail: zhangyp@wzu.edu.cn
Received: 18 October 2014 Accepted: 19 January 2015

of *Lygodactylus picturatus*, *Hemidactylus frenatus*, *Hemidactylus mabouia*, and *Tarentola mauritanica* while Phillips and Asa (1993) reported the development of the midpiece section in *Sphaerodactylus cinereus*. Jamieson *et al*. (1996) has detailed study of the ultrastructure of spermatozoa of *Heteronotia binoei* and Röll and von Düring (2008) investigated the difference in the spermiogenesis of the normal and the phenotypic males. Rheubert *et al*. (2011) provided a detailed description of the formation of the sperm of *Hemidactylus turcicus*. There is a need for additional ultrastructural spermatozoa studies to develop a comprehensive phylogenetic hypothesis for this family.

Gekko japonicus, Gekko chinensis and Hemidactylus bowrigii in our study are all oviparous and nocturnal animals. *G. japonicus* mainly distributes in the south of the Huaihe, west to Shanxi and Gansu in China, but also in Japan and Korea. *G. chinensis* is the endemic species of China, living in the wild or the structure gaps in Fujian, Guangdong, Hainan, Guangxi, while *H. bowrigii* distributes mainly in Fujian, Hainan, Sichuan, Guangdong, Guangxi, Taiwan and Yunnan in China, and is also common in India, Sikkim, Burma and Ryukyu islands in Japan (Zhao *et al.* 1999). Here we provided a detailed description of the mature spermatozoa of *G. japonicus*, *G. chinensis* and *H. bowrigii* for the first time. Our results were compared with the mature spermatozoa of previously examined gecko species. The main objectives of this study were to understand the spermatozoal autapomorphies in the family Gekkonidae and to provide a theoretical basis for detailed phylogenetic study on Gekkonidae. Specifically, we ascertained the degree of variability in sperm morphology of three Gekkonidae species common in China.

2. Materials and Methods

Mature spermatozoa from male *G. japonicus*, *G. chinensis* and *H. bowrigii* were collected from animals captured in three locations in China: Wenzhou, Zhejiang (27°23' N, 119°37' E), Quanzhou (24°30' N, 117°27' E) and Putian (25°45' N, 119°03' E), Fujian. All lizards used in this study were captured in early May 2014.

Four adult specimens of each species were quickly sacrificed in the laboratory. Epididymides of each experimental lizard were removed, and diced into 1–2 mm^3 pieces and placed in a petri dish with phosphate-buffered saline solution (PBS, pH 7.2). A small part of epididymides sample for sperm smear analysis was fixed using a solution containing 2.5% glutaraldehyde, 2% paraformaldehyde and 3% sucrose in 0.1M sodium cacodylate buffer, pH 7.2, for 10 min. Once fixed, each sample was stained for 30 s withtoluidine blue under an alcohol lamp. The morphology of entire sperm was observed under a light microscope (Olympus BX51, Japan) and morphological features were digitally captured with a CCD camera (Olympus DP71, Japan). Lengths of the head, midpiece and entire sperm of the three species were measured with a micrometer under the light microscope (Olympus BX51, Japan). The descriptions of sperm ultrastructure were based on the protocol described for the saurians (Colli *et al.*, 2007; Giugliano *et al.*, 2002; Jamieson *et al.*, 1996; Scheltinga *et al.*, 2001).

The rest of the epididymides samples were fixed at 4°C overnight using 2.5% glutaraldehyde solution. Tissue samples were then rinsed in 0.1M phosphate buffer at pH 7.2, post-fixed for 1h in buffered 1% osmium tetroxide, rinsed in 0.1M phosphate buffer, dehydrated through series of ascending contents of acetone (70–100%) and then finally embedded in epoxy resin. Ultrathin sections prepared by microtome were stained for 30 s in lead citrate, rinsed in distilled water, then in 6% aqueous uranyl acetate for 4 min, rinsed in distilled water, and further stained for 2 min in lead citrate before final rinse with distilled water. Electron micrographs were taken on a Hitachi 7500 transmission electron microscope (TEM). Using the TEM, the following morphometric were determined for each species following the techniques suggested by Teixeira *et al*. (2002) and Zhang *et al*. (2006): the length of perforatorium, midpiece, acrosome, nuclear rostrum, the width of nuclear shoulder and nuclear base. We used one-way analysis of variance (ANOVA) to statistically compare the various morphometric parameters (e.g., length of mid-piece, width of nucleus shoulder) of sperm collected from these three groups of Gekkonidae used in the study. Post-hoc comparisons of significantly different ($P < 0.05$) parameters were conducted by the Tukey's test using Statistica version 6.0.

3. Results

3.1 Spermatozoal morphometrics Main sperm morphological dimensions and the statistical results of the three species of Gekkonidae are shown in Table 1. The total length ($F_{2,57} = 23.66$, $P < 0.0001$), head length ($F_{2,43} = 4.64$, $P < 0.05$) and nuclear base width ($F_{2,22} = 3.97$, $P < 0.05$) of the spermatozoa were significantly different among species. *G. japonicus* had significantly shorter sperm than *G. chinensis* and *H. bowrigii*. The head length and nuclear base width follow the trend *G. japonicus* >

G. chinensis > *H. bowrigii*. *H. bowrigii* had significantly longer midpiece than *G. chinensis* and *G. japonicus* ($F_{2,33}$ = 23.66, $P < 0.01$). There were no statistical differences between any of the three species in the length of perforatorium ($F_{2,10}$ = 1.62, P = 0.25), acrosomal complex ($F_{2,10}$ = 0.34, P = 0.72) and nuclear rostrum ($F_{2,18}$ = 1.89, P = 0.18) or the width of nuclear shoulder ($F_{2,20}$ = 0.34, P = 0.72).

3.2 Ultrastructure of spermatozoa Spermatozoa of *G. japonicus* (Figure 1A), *G. chinensis* (Figure 1B) and *H. bowrigii* (Figure 1C) are filiform cells, consisting of head, midpiece and tail. The head is made up of acrosomal complex and the nucleus (Figures 2A; 4A and 6A) while the tail is subdivided into principal piece and endpiece (Figures 3E; 5F and 7N).

Acrosome complex In all three species, the acrosomal complex has a coniform and slightly curved shape and is composed of two caps: an external acrosomal vesicle and an internal subacrosomal cone. The acrosomal vesicle is the anterior terminal portion of the spermatozoon, also called acrosomal cap, which is distinctly divided into an external, moderately electrodense and thin cortex, and an internal denser medulla (Figures 2A, B, K; 4A, B, C; and 6A, B, G). Cross striations are seen in concentric circles (Figures 2B; 4C; and 6B). The posterior of acrosomal vesicle is very thin and sleeve-shaped, hence it is often referred to as acrosomal sleeve (Figures 2A; 4A, B; and 6A). Within the acrosomal medulla, the subacrosomal space contains a perforatorium that resembles a very narrow elongated cone with a pointed tip (Figures 2A, C, K; and 4B, C). The perforatorium begins at a stopper-like perforatorial base plate, embedded in the apex of the subacrosomal cone (Figures 2A, D; 4A, D; and 6G). The subacrosomal cone surrounds the tapered anterior end of the nucleus (Figures 2A, 4A, B; and 6A, G). There is a slightly densified subacrosomal space between the base of the perforatorium and the anterior extremity of the subacrosomal cone (Figures 2A; 4A, B; and 6A, G). The transverse sections of acrosomal vesicle are rounded. In *G. japonicus* and *G. chinensis*, an epinuclear electron-lucent zone is present within the anterior region of the subacrosomal cone immediately anterior to the nuclear

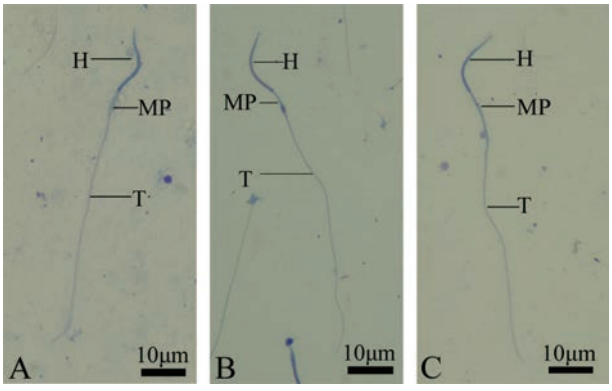

Figure 1 Light microscope photographs of spermatozoa. A, B and C are light micrographs of the entire spermatozoa of *Gekko japonicus*, *Gekko chinensis* and *Hemidactylus bowrigii*, respectively. H: head; MP: midpiece; T: tail.

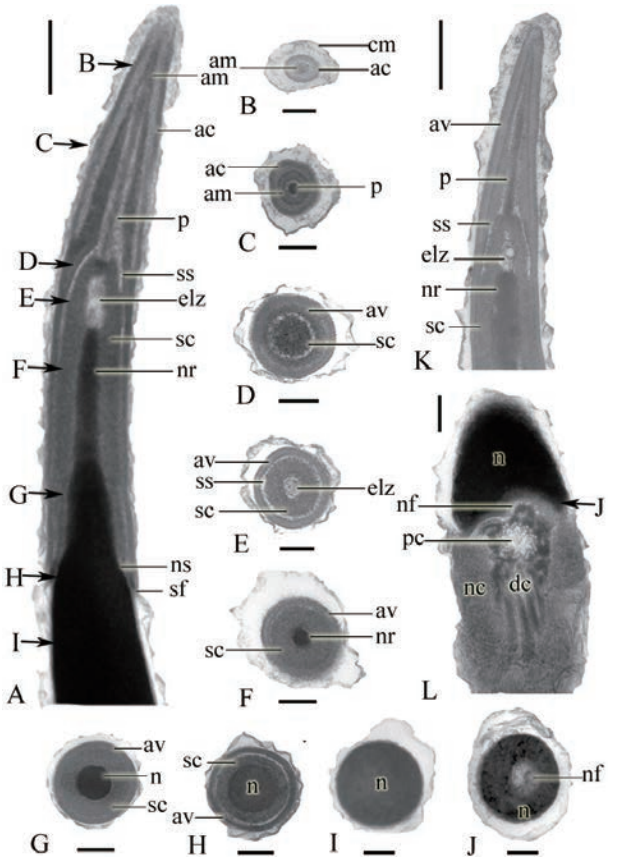

Figure 2 Sperm head of *Gekko japonicus*. (A) Longitudinal section(LS) of the head showing the acrosomal cortex, acrosomal medulla, perforatorium, subacrosomal cone, subacrosomal space, perforatorium base plate, epinuclear lucent zone, nuclear rostrum, flage of subacrosomal material, nuclear shoulder and nucleus. (B–J) A series of transverse sections (TS) through the spermatozoon as indicated. (B) acrosomal vesicle. (C) perforatorium. (D) subacrosomal cone. (E) epinuclear lucent zone. (F) beginning of the nuclear rostrum. (G) nuclear rostrum. (H) nuclear shoulder. (I) nucleus. (J) nuclear fossa. (K) LS of the acrosomal complex showing acrosomal cortex, perforatorium, subacrosomal cone, subacrosomal space and epinuclear lucent zone. (L) LS of the neck region showing fossa, dense collar, proximal centriole and distal centriole. (A) and (K) scale bar 0.5 μm; (B)–(J) and (L) scale bar 0.2 μm. ac: acrosomal cortex, am: acrosomal medulla, cd: central dense body, dc: distal centriole, elz: epinuclear lucent zone, nc: dense collar, mi: mitochondria, ls: laminar structure, nf: nuclear fossa, nr: nuclear rostrum, p: perforatorium, pb: perforatorium base plate, pc: proximal centriole, pcm: pericentriolar material, pf: postero-lateral flange, sc: subacrosomal cone, sf: flage of subacrosomal material, ss: subacrosomal space.

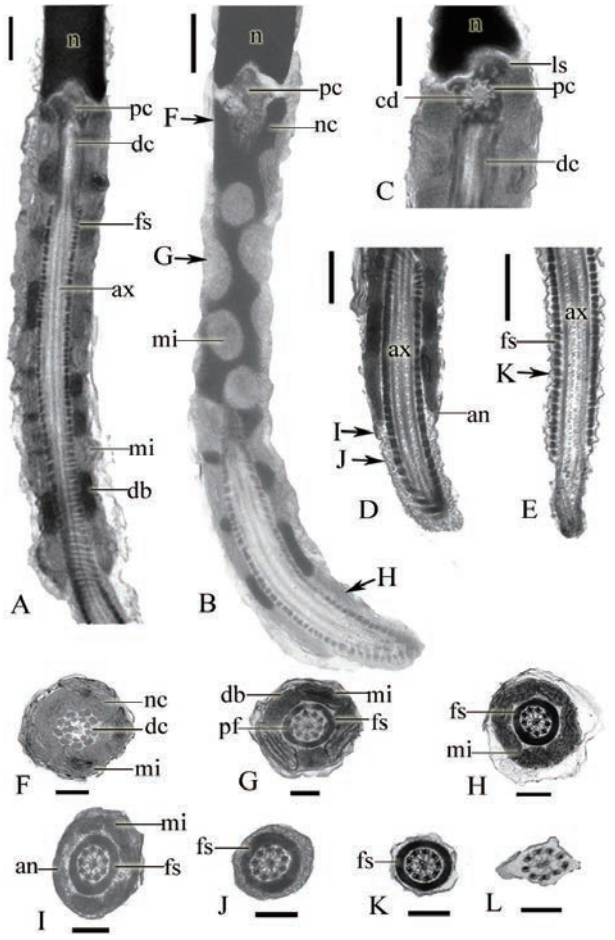

Figure 3 Sperm tail of *Gekko japonicus*. (A) Longitudinal section (LS) of the neck region and midpiece showing nucleus, nuclear fossa, proximal centriole, distal centriole, neck cylinder, axoneme, fibrous sheath, and mitochondria. (B) LS of the neck region and midpiece showing proximal centriole, neck cylinder and the dense body and mitochondrial arrangement. (C) LS of the neck region showing the laminar structure, proximal centriole and distal centriole. (D) LS of the posterior region of the midpiece and the anterior region of the principal piece, showing annulus and axoneme. (E) LS of the posterior region of the principal piece and the endpiece showing axoneme and fibrous sheath. (F) LS of the neck region, showing proximal centriole, distal centriole and fibrous sheath. (G) Transverse section (TS) through the midpiece, showing dense body, mitochondria and axoneme. (H) TS of the midpiece before the aunulus, showing mitochondria and axoneme. (I) TS through the annulus, showing annulus, mitochondria and axoneme. (J) TS through the anterior region of the principal piece showing axoneme. (K) LS of the principal piece showing axoneme. (L) TS of the endpiece. (A)–(E) scale bar 0.5 μm; (F)–(L) scale bar 0.2 μm. an: annulus, ax: axoneme, db: dense body, cd: central dense body, dc: distal centriole, fs: fibrous sheath, ls: laminar structure, mi: mitochondria, n: nucleus, nc: neck cylinder, pc: proximal centriole, pf: peripheral fibers 3 and 8.

rostrum, while in *H. bowrigii* it is beginning at the tip of the nuclear space (Figures 2A, E, K; 4A, E; and 6C, G). However, the shape of epinuclear electron-lucent zone differs among the three species. *G. japonicus* is short rod-

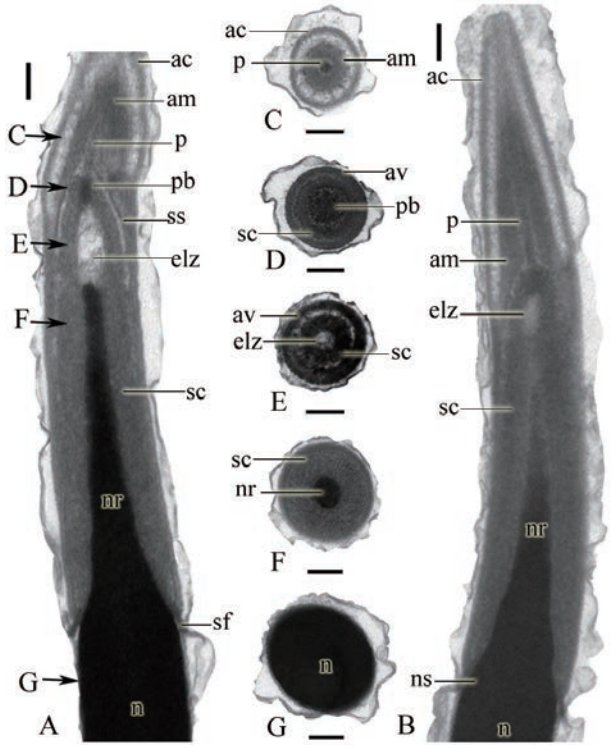

Figure 4 Sperm head of *Gekko chinensis*. (A) and(B) Longitudinal section (LS) of the anterior region of the head showing the acrosomal vesicle, perforatorium, perforatorium base plate, subacrosomal cone, subacrosomal space, nuclear rostrum, flage of subacrosomal material, epinuclear lucent zone, nuclear shoulder and nucleus. (C–G) A series of transverse sections (TS) through the spermatozoon as indicated. (C) perforatorium. (D) perforatorium base plate. (E) epinuclear lucent zone. (F) nuclear rostrum. (G) nucleus. (A)–(G) scale bar 0.2 μm. ac: acrosomal cortex, am: acrosomal medulla, dc: distal centriole, elz: epinuclear lucent zone, nc: neck cylinder, mi: mitochondria, ls: laminar structure, nf: nuclear fossa, nr: nuclear rostrum, p: perforatorium, pb: perforatorium base plate, pc: proximal centriole, pcm: pericentriolar material, pf: postero-lateral flange, sc: subacrosomal cone, sf: flage of subacrosomal material, ss: subacrosomal space.

like with low electron density, *G. chinensis* is fusiform while *H. bowrigii* is long rod-like with high electron density. The nuclear space from the anterior to the nuclear rostrum in *H. bowrigii* was not observed in other two species that we examined (Figure 6G).

Nucleus The nucleus is elongated and composed of highly condensed, electron-dense chromatin. In transverse section, the nucleus is circular (Figures 2I, J; 4G; and 6E, F). Nucleus anteriorly tapers to form a slender cone, called nuclear rostrum, within the acrosome complex (Figures 2A; 4A, B; and 6A). Rounded nuclear shoulder is observed at the basal end of the rostrum (Figures 2A; 4B; and 6A). Nuclear shoulder has a diameter slightly smaller than the base of the nucleus. The basal pole of the nucleus has a conical depression called the nuclear fossa or implantation fossa associated with the neck elements

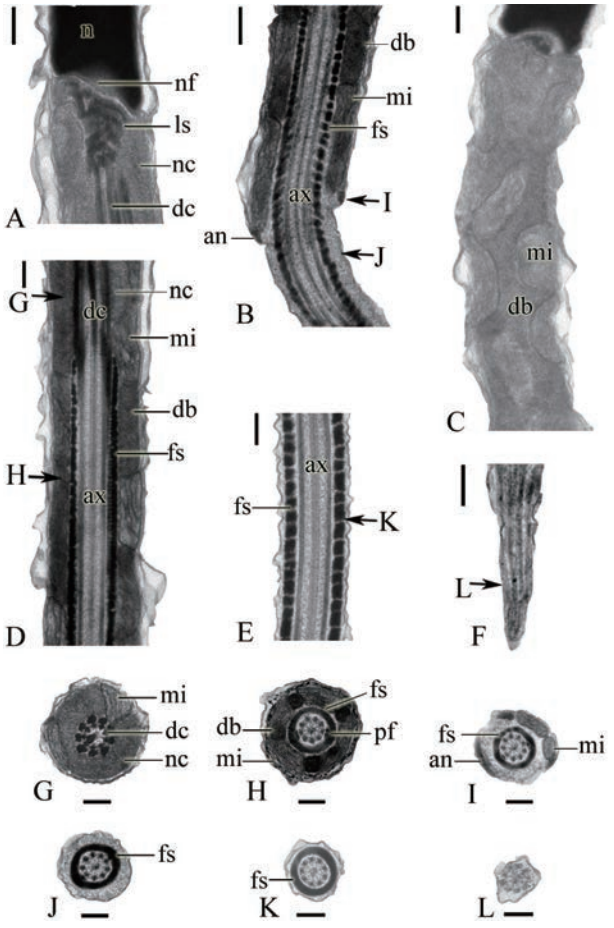

Figure 5 Sperm tail of *Gekko chinensis*. (A) Oblique longitudinal section (LS) of the neck, presenting laminar structure, neck cylinder and distal centriole. (B) LS of the posterior region of the midpiece showing annulus. (C) Oblique LS of the midpiece showing the mitochondrial and dense body arrangement. (D) LS of the neck and midpiece, showing neck cylinder, axoneme, fibrous sheath, dense body and mitochondria. (E) LS of the principal piece, showing fibrous sheath and axoneme. (F) LS of the endpiece. (G–L) A series of transverse sections (TS) through the spermatozoon as indicated. (G) neck. (H) midpiece. (I) annulus. (J) anterior region of the principal piece. (K) principal piece. (L) endpiece. (A)–(L) scale bar 0.2 μm. an: annulus, ax: axoneme, db: dense body, dc: distal centriole, fs: fibrous sheath, ls: laminar structure, mi: mitochondria, n: nucleus, nc: neck cylinder, pc: proximal centriole, pf: peripheral fibers 3 and 8.

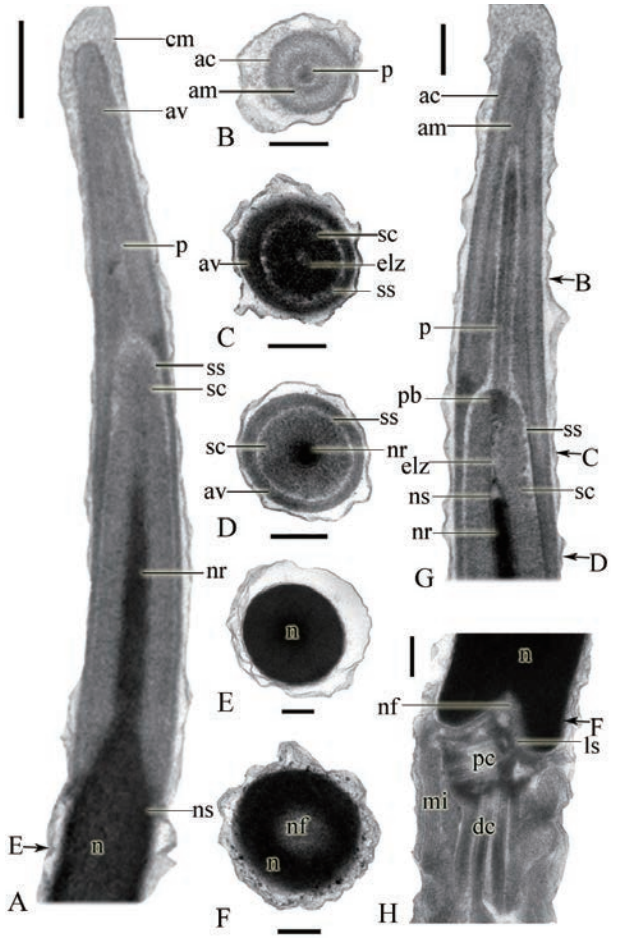

Figure 6 Sperm head of *Hemidactylus bowrigii*. (A) Longitudinal section (LS) of the anterior region of the head showing the acrosomal vesicle, perforatorium, subacrosomal cone, subacrosomal space, nuclear rostrum, flage of subacrosomal material, nuclear shoulder and nucleus. (B) Transverse section (TS) through the perforatorium. (C) TS through the epinuclear lucent zone. (D) TS through the nuclear rostrum. (E) TS through the nucleus. (F) Transverse section through the nuclear fossa. (G) LS of the acrosomal complex. (H) LS of the posterior region of the head and the neck. (A) scale bar 0.5 μm; (B)–(F) scale bar 0.2 μm. ac: acrosomal cortex, am: acrosomal medulla, dc: distal centriole, elz: epinuclear lucent zone, nc: neck cylinder, mi: mitochondria, ls: laminar structure, nf: nuclear fossa, nr: nuclear rostrum, ns: nuclear space, p: perforatorium, pb: perforatorium base plate, pc: proximal centriole, pcm: pericentriolar material, pf: postero-lateral flange, sc: subacrosomal cone, sf: flage of subacrosomal material, ss: subacrosomal space.

(Figures 2L, J; and 6F, H).

Neck region The neck region occurs at the junction between nucleus and midpiece. It includes proximal and distal centrioles, neck cylinder or dense collar and mitochondria (Figures 2L; 3C; 5A; and 7A, I). The proximal centriole is located before the distal centriole, and it lies at approximately 90° to the distal centriole. The proximal centriole has nine short microtubule triplets arranged in a circular pattern (Figures 3C; and 7L). Electron-densed lamellar structures that are associated with pericentriolar material lie on both sides in the front of the proximal centriole (Figures 3C; 5A; 6H; and 7A, L). The distal centriole forms the basal body or basal granule of the axoneme and is characterized by the presence of a central electron-dense body (Figures 3F; 5G; and 7C, D). Nine triplets of microtubules and a pair of central microtubules from the axoneme are observed in a distal centriole. Nine peripheral fibers that partially cover each triplets and a central fiber connected to the central

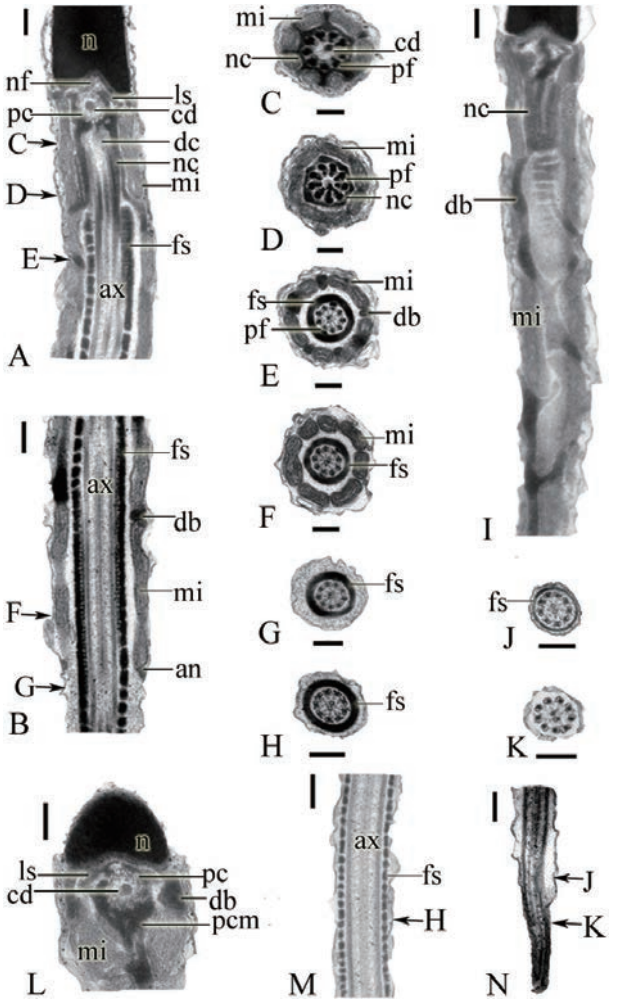

Figure 7 Sperm tail of *Hemidactylus bowrigii*. (A) Longitudinal section (LS) of the neck showing nucleus, nuclear fossa, laminar structure, proximal centriole, distal centriole, central dense fibrous, neck cylinder, axoneme, fibrous sheath, and mitochondria. (B) LS of the posterior region of the midpiece and the anterior region of the principal piece, showing annulus and axoneme. (C–H, J, K) A series of transverse sections (TS) through the spermatozoon as indicated. (C and D) neck. (E) midpiece. (F) midpiece before the aunulus. (G) anterior region of the principal piece. (H) principal piece. (I) Oblique LS of the neck and the anterior region of the midpiece showing neck cylinder and the arrangement of dense body and mitochondrial. (J) TS through the posterior region of the principal piece. Here the fibrous sheath is very thin. (K) TS of the endpiece. And the fibrous sheath is disappeared. (L) LS of the neck showing laminar structure, proximal centriole, distal centriole, pericentriolar material, dense body and mitochondria. (M) LS of the principal piece, showing axoneme. (N) LS of the posterior region of the principal piece and the endpiece. (A)–(N) scale bar 0.2 μm. an: annulus. ax: axoneme, db: dense body, cd: central dense body, dc: distal centriole, fs: fibrous sheath, ls: laminar structure, mi: mitochondria, n: nucleus, nc: neck cylinder, pc: proximal centriole, pf: peripheral fibers 3 and 8.

microtubule are present. A special structure observed in all three species is the neck cylinder. However, the neck cylinders of different species have their distinct characteristics. The neck cylinders of *G. japonicus* and *G. chinensis* are thick, 0.19 μm and form a ring structure in cross-section containing a few mitochondria (Figures 3F; and 5G), while that of *H. bowrigii* is very thin, about 0.02 μm and looks like a seven-pointed star in cross-section. Besides, around the neck cylinder of *H. bowrigii*, there are seven mitochondria (Figures 7C, D).

Midpiece The midpiece of *G. japonicus*, *G. chinensis* and *H. bowrigii* begins with the neck cylinder and ends with the annulus. It includes the neck region, axoneme surrounded by mitochondrial sheath and the fibrous sheath (Figures 3A, B; 5B; and 7A, B, I).

The mitochondrial sheath surrounds the fibrous sheath and is composed of mitochondria and dense bodies arranged in grid. The mitochondria are in meshes formed by the dense bodies (Figures 3B; 5C; and 7I). In the species of *G. japonicus* and *G. chinensis*, the mitochondria are ovoid in oblique section while in *H. bowrigii*, the mitochondria have irregular shape. In transverse section, mitochondria are ovoid in shape composed of linear cristae (Figures 3G; 5H; and 7E). In addition, there are seven mitochondria without dense bodies before the annulus (Figures 3H; and 7F). The small ovoid annulus lies in the end of the midpiece and is close to the inner surface of the cell membrane (Figures 3D, I; 5B, I; and 7B). Axoneme is enclosed by the fibrous sheath that begins at the base of the distal centriole and extends into the midpiece (Figures 3A, G, H; 5D, H; and 7A, B E). Fibrous sheath appears as ring structures of dense material in transverse sections, and has regular shape composed of neatly arranged squares when viewed in the longitudinal section. Axoneme complex is composed of a pair of central microtubules (singlets) surrounded by nine doublets of microtubules associated with nine peripheral dense fibers (Figures 3A, G; 5D, H; and 7B). A central fiber connects with the two singlets, which posteriorly diminishes in size and is located centrally between the singlets of the axoneme. The central fiber is vestigial and not observable at the level of the granular cytoplasmic zone (Figures 3J; 5J; and 7G). In all species, the diameter of peripheral fibers rapidly decrease posteriorly except for the fibers at doublets 3 and 8 that form a double structure separated from their corresponding doublet and closely associated with the fibrous sheath (Figures 3G, H; 5H; and 7E, F). Posterior to the granular cytoplasmic zone, all nine peripheral fibers are vestigial or absent. The fibers at doublets 3 and 8 are absent at the anterior of the principal piece, which is the granular cytoplasmic zone (Figures 3J; 5J; and 7G).

Principal piece In all three species, the principal

piece has similar structure and is the longest part of the spermatozoon and occurs behind the midpiece. It consists of the axoneme surrounded by fibrous sheath, cytoplasm, and plasma membrane (Figures 3J, K; 5E, K; and 7H, M). In the anterior portion of the principal piece and immediately after the annulus, the diameter of the spermatozoon does not decrease compared to the annulus diameter and a thick region of granular cytoplasm widely separates the plasma membrane from the fibers sheath (Figures 3D; 5B; and 7B). Posteriorly, the plasma membrane becomes closely attached to the fibrous sheath (Figures 3E; 5E; and 7M). The thickness of the fibrous sheath becomes thinner and thinner and disappeared the junction with the endpiece, while the 9 + 2 pattern of the axonemal microtubules remains unaltered (Figure 7J).

Endpiece The three species have endpiece with similar structure. It is a short axoneme extending beyond the posterior limit of the fibrous sheath (Figures 3E; 5F; and 7N). The length of the endpiece is difficult to measure because the fiber sheath disappears and only the plasma membrane was observable. In the proximal section, the axoneme is still visible with the "9 + 2" structure that gradually becomes disrupted and shows irregular arrangement (Figures 3L; 5L; and 7K).

4. Discussion

4.1 Synapomorphies of the family Gekkonidae

The spermatozoa of *G. japonicus*, *G. chinensis* and *Hemidactylus bowrigii* exhibit the following squamate synapomorphies: a acrosomal vesicle and subacrosomal cone; a single prenuclear perforatorium; absence of endonuclear canal; presence of a nucleus rostrum and intermitochondrial dense bodies; linear mitochondrial cristae; fibers at doublets 3 and 8 are thick and form a double structure separated from their corresponding doublet and fibrous sheath extending into midpiece but not into the neck region (Jamieson, 1995; Jamieson *et al.*, 1996; Jamieson and Healy, 1992; Giugliano *et al.*, 2002; Oliver, 1996; Teixeira *et al.*, 1999b, c; Teixeira *et al.*, 2002; Vieira *et al.*, 2004; Zhang *et al.*, 2006). Furthermore, rounded nuclear shoulder, a perforatorial base-plate, subacrosomal space were observed in the three species and all the gekkonid lizards reported (Furieri, 1970; Jamieson *et al.*, 1996; Rheubert *et al.*, 2011). The neck cylinder with mitochondria and dense

Table 1 Sperm morphological dimensions of the three species of Gekkonidae

Regions	*Gekko japonicus*	*Gekko chinensis*	*Hemidactylus bowrigii*
TL (μm)	74.81 ± 1.91 [b] (71.28–78.00) (*n* = 20)	82.28 ± 3.65 [a] (76.25–88.00) (*n* = 20)	79.94 ± 4.50 [a] (71.75–90.25) (*n* = 20)
HL (μm)	15.39 ± 1.18 [a] (13.55–17.71) (*n* = 14)	14.58 ± 1.40 [ab] (12.38–18.86) (*n* = 17)	13.83 ± 1.43 [b] (*n* = 11.25–15.00) (*n* = 15)
AL (μm)	3.80 ± 0.28 (3.44–4.13) (*n* = 4)	3.88 ± 0.09 (3.80–4.01) (*n* = 4)	3.72 ± 0.29 (3.35–4.06) (*n* = 5)
PL (μm)	1.10 ± 0.12 (0.92–1.21) (*n* = 5)	1.10 ± 0.37 (1.00–1.19) (*n* = 5)	0.97 ± 0.06 (0.91–1.03) (*n* = 3)
*N*RL (μm)	1.66 ± 0.24 (1.26–1.93) (*n* = 8)	1.82 ± 0.11 (1.68–2.03) (*n* = 8)	1.75 ± 0.12 (1.64–1.89) (*n* = 5)
MPL (μm)	5.76 ± 0.81 [b] (4.82–8.06) (*n* = 14)	6.45 ± 0.37 [b] (6.12–7.06) (*n* = 6)	14.17 ± 1.54 [a] (12.50–16.25) (*n* = 16)
*N*SW (μm)	0.50 ± 0.15 (0.38–0.89) (*n* = 9)	0.52 ± 0.04 (0.46–0.58) (*n* = 8)	0.45 ± 0.04 (0.40–0.52) (*n* = 6)
*N*BW (μm)	0.73 ± 0.08 [a] (0.52–0.81) (*n* = 15)	0.70 ± 0.04 [ab] (0.64–0.75) (*n* = 4)	0.63 ± 0.07 [b] (0.51–0.71) (*n* = 6)

Note: All values are expressed as Mean ± SD. Content in parentheses represents the range and degrees of freedom. Means superscripted with different letters are significantly different (Tukey's posthoc test, α= 0.05; a > b). TL: total sperm length, HL: head length, AL: acrosome length, PL: perforatorium length, NRL: nuclear rostrum length, MPL: midpiece length, NSW: nuclear shoulders width, NBW: nucleus base width.

bodies arranged in grid with mitochondria were also observed in the three species, which were accordance to the Jamieson's report (Jamieson *et al.*, 1996). The similar results were observed in Furieri's research about *Hemidactylus frenatus, L. picturatus and T. mauritanica* (Furieri, 1970). Hence, we concluded that the rounded nuclear shoulder, a perforatorial base-plate, subacrosomal space, the neck cylinder with mitochondria and dense bodies arranged in grid with mitochondria are synapomorphies of Gekkonidae. In lizards other than Gekkonidae, such as Tropiduridae, Phrynosomatidae, Polychrotidae, Crotaphytidae, Agamidae, Chamaeleonidae (Scheltinga *et al.*, 2001), Hoplocercidae, Opluridae (Vieira *et al.*, 2007), Varanidae (Oliver, 1996), Lacertidae (Zhang *et al.*, 2005) and Scincidae (Liu and Zhang, 2004; Zhang *et al.*, 2006), the neck cylinder with mitochondria and dense bodies arranged in grid with mitochondria have not been reported. Although the neck cylinder surrounding the distal centriole has been observed in serpents, there is no inset mitochondria around it (Colli *et al.*, 2007; Cunha *et al.*, 2008; Oliver *et al.*, 1996; Tavares-Bastos *et al.*, 2008; Tourmente *et al.*, 2006; Teixeira *et al.*, 2002; Vieira *et al.*, 2007). In the midpiece, zigzagged mitochondria are tightly arranged and the dense body is scarce and even absent (Cunha *et al.*, 2008; Jamieson and Koehler, 1994; Oliver *et al.*, 1996; Tavares-Bastos *et al.*, 2008; Tourmente *et al.*, 2008; Tourmente *et al.*, 2006). Therefore, our results showed that neck cylinder with mitochondria and dense bodies arranged in grid with mitochondria are autapomorphies of Gekkonidae.

4.2 Polymorphic characters among the Gekkonidae species Our research, as well as previous studies on spermatozoa ultrastructure of Gekkonidae shows several distinct features in spermatozoa ultrastructure of the different species (Table 2). The subacrosomal cone in cross-section of *Heteronotia binoei* (Jamieson *et al.*, 1996) is apically quadrangular rather than circular like observed in other species. The epinuclear electron-lucent zone is absent in *Hemidactylus frenatus* and *Heteronotia binoei* (Furieri, 1970; Jamieson *et al.*, 1996) short, rod-shaped and low electron dense in *G. japonicus*, fusiform in *G. chinensis* and is long, rod-like and highly electron-dense in *Hemidactylus bowrigii*. The nuclear space is only observed in *Hemidactylus bowrigii* and not in others of Gekkonidae species. However, this nuclear space structure has been reported in four species of *Tupinambis* (Tavares-Bastos *et al.*, 2002) and some serpents, such as *Epicrates cenchria*, *Boa constrictor amarali*, and *Corallus hortulanus* (Tavares-Bastos *et al.*, 2008). Furthermore, the neck cylinders of *G. japonicus* and *G. chinensis* are thick and ring-shaped with few mitochondria in cross-section while those of *Hemidactylus bowrigii* and *Heteronotia binoei* are thin. In *Hemidactylus bowrigii*, the neck cylinder is like a seven-pointed star surrounded by seven mitochondria while in *Heteronotia binoei*, it is arranged as a six- or seven-pointed star surrounded by more mitochondria

Table 2 Variability of spermatozoa ultrastructure among different species of Gekkonidae

Species	Subacrosomal cone point in transverse section	Epinuclear electron-lucent zone	Nuclear space	neck cylinder shape in transverse section	neck cylinder shape in longitudinal section	Laminar structure	Mitochondrial number in transverse section of the midpiece	Mitochondrial shape in oblique section of the midpiece	Reference
Gekko japonicus	Circular	Present	Absent	Ring structure	Thick	Present	3–4	Ovoid	This study
Gekko chinensis	Circular	Present	Absent	Ring structure	Thick	Present	5	Ovoid	This study
Hemidactylus bowrigii	Circular	Present	Present	Sven-pointed star	Thin	Present	6	Anomalous	This study
Hemidactylus turcicus	Circular	Present	absent	Unknown	Unknown	Unknown	6	Unknown	Rheubert *et al.*, 2011
Hemidactylus frenatus	Circular	Absent	Absent	Unknown	Unknown	Unknown	6	Ovoid	Furieri, 1970
Heteronotia binoei	Quadrangular	Absent	Absent	Six- or seven-pointed star	Thin	Absent	9	Anomalous	Jamieson *et al.*, 1996
Lygodactylus picturatus	Circular	Present	Absent	Unknown	Unknown	Unknown	3	Anomalous	Furieri, 1970
Tarentola mauritanica	Circular	Present	Absent	Unknown	Unknown	Unknown	5	Unknown	Furieri, 1970

(Jamieson *et al.*, 1996). The laminar structure observed in *G. chinensis*, *G. japonicus* and *Hemidactylus bowrigii* is absent in *Heteronotia binoei* (Jamieson *et al.*, 1996). In oblique section of the midpiece, mitochondria are ovoid in *G. japonicus*, *G. chinensis* and *Hemidactylus frenatus*, but are anomalous in *Hemidactylus Bowrigii*, *Heteronotia binoei* and *Lygodactylus picturatus* (Furieri, 1970; Jamieson *et al.*, 1996). In addition, the mitochondrial abundance of different Gekkonidea species varies from 3 to 9 in transverse section of the midpiece with notable three species of *Hemidactylus* containing 6 (Furieri, 1970; Jamieson *et al.*, 1996; Rheubert *et al.*, 2011). The midpiece lengths of *G. japonicus* (5.77 μm) and *G. chinensis* (6.45 μm) are very much shorter than *Hemidactylus bowrigii* (14.28 μm).

The polymorphic traits in sperm ultrastructure among congeneric species had been documented in lizards such as Crotaphytidae(Scheltinga *et al.*, 2001), Polychrotidae (Teixeira *et al.*, 1999a ; Scheltinga *et al.*, 2001) and Tropiduridae (Teixeira *et al.*, 1999d). Polymorphic characters commonly occur in the acrosome complex and midpiece, which are believed to be influenced by the fertilization processes and physiological environment demands. In fertilization processes, acrosome aids the sperm to penetrate the ovum using energy provided by the midpiece section. However, spermatozoa of different species have to acclimatize to various fertilization conditions including the penetration of various kinds of egg envelopes (Tavares-Bastos *et al.*, 2002). Therefore, the knowledge on polymorphism of sperm ultrastructure can improve the veracity of the phylogenetic analysis, and it has great value on comparative biology, phylogenetic reconstruction, and evolution history.

4.3 Concluding remarks The sperm ultrastructure characteristics such as the shape of subacrosomal cone point in transverse section, the presence or absence of nuclear space and laminar structure, the shape of the epinuclear electron-lucent zone, the structure of the neck region and the forms of the mitochondria in the midpiece, and the sperm dimensions have certain intergeneric and interspecific differences. These features can cast light on the phylogenetic relationships of Gekkonidae. In addition, detailed description of the spermatozoa ultrastructure and statistical analyses of sperm dimensions of Gekkonidae provide quantitative estimates of the degree of variability in sperm ultrastructure between different genera in Gekkonidae. Moreover, our results provide basic information that are of value for further studies on molecular mechanism of reptile spermatogenesis.

For future study, the molecular mechanism of reptile spermatogenesis should be emphasized. Spermatogenesis is a complex process where spermatogonia undergo mitotic, meiotic, morphological transformations to finally become a functional mature sperm (Hou and Yang, 2013). There are three important steps in this process which include acrosome formation, nuclear shaping and flagellum formation (Hu *et al.*, 2012; Hu *et al.*, 2013). Future studies should include the following topics: formation of acrosome; factors affecting nuclear elongation; composition and function of motor protein and cytoskeleton during spermatogenesis of reptile.

Acknowledgements We thank Joselito M. Arocena, the full professor of University of Northern British Columbia, for his help in polishing the language of our manuscript. Our experimental procedures complied with the current laws on animal welfare and research in China. This work was supported by the grants from the National Natural Science Foundation of China (31170376).

References

Cunha L. D., Tavares-Bastos L., Báo S. N. 2008. Ultrastructural description and cytochemical study of the spermatozoon of *Crotallus durissus* (Squamata, Serpentes). Micron, 39: 915–925

Colli G. R., Teixeira R. D., Scheltinga D. M., Mesquita D. O., Wiederhecker H. C., Báo S. N. 2007. Comparative study of sperm ultrastructure of five species of teiid lizards (Teiidae, Squamata), and *Cercosaura ocellata* (Gymnophthalmidae, Squamata). Tissue Cell, 39: 59–78

Furieri P. 1970. Sperm morphology of some reptiles: Squamata and Chelonia. In Baccetti B. (Ed.), *Comparative Spermatology*. Rome: Accademia Nazionale dei Lincei, 115–131

Giugliano L. G., Teixeira R. D., Colli G. R., Báo S. N. 2002. Ultrastructure of spermatoxoa of the Lizard *Ameiva ameiva*, with considerations on polymorphism within the Family Teiidae (Squamata). J Morph, 253: 264–271

Hu J. R., Liu M., Wang D. H., Hu Y. J, Tan F. Q., Yang W. X. 2013. Molecular characterization and expression analysis of a KIFC1-like kinesin gene in the testis of *Eumeces chinensis*. Mol Biol Rep, 40: 6645–6655

Hu J. R., Xu N., Tan F. Q., Wang D. H., Liu M., Yang W. X. 2012. Molecular characterization of a KIF3A-like kinesin gene in the testis of the Chinese fire-bellied newt *Cynops orientalis*. Mol Biol Rep, 39(4): 4207–4214

Hou C. C., Yang W. X. 2013. Acroframosome-dependent KIFC1 facilitates acrosome formation during spermatogenesis in the caridean shrimp *Exopalaemon modestus*. PloS ONE, 8(9): 1–16

Han D. M., Zhou K. Y., Bauer A. M. 2004. Phylogenetic relationships among gekkotan lizards inferred from C-mos nuclear DNA sequences and a new classification of the Gekkota. Biol J Linn Soc, 83: 353–368

Jamieson B. G. M. 1995. The ultrastructure of spermatozoa of the Squamata (Reptilia) with phylogenetic considerations. In Jamieson B. G. M., Ausio J., Justine J. (Eds.), Advances

in Spermatozoal Phylogeny and Taxonomy. Paris: Muséum National d'Histoire Naturelle, 359–383

Jamieson B. G. M., Healy J. M. 1992. The phylogenetic position of the tuatara *Sphenodon* (Sphenodontida, Amniota), as indicated by cladistic analysis of the ultrastructure of spermatozoa. Philos Trans R Soc London (B), 335: 207–219

Jamieson B. G. M., Koehler L. 1994. The ultrastructure of the spermatozoon of the northern water snake, *Nerodia sipedon* (Colubridae, Serpentes), with phylogenetic considerations. Can J Zool, 72: 1648–1652

Jamieson B. G. M., Oliver S. C., Scheltinga D. M. 1996. The ultrastructure of spermatozoa of Squamata, I, Scincidae, Gekkonidae and Pygopodidae (Reptilia). Acta Zool, 77: 85–100

Liu Y. Z., Zhang Y. P. 2004. Ultrastructure of spermatozoa of *Eumeces elegans*. Zool Res, 25(5): 429–435 (In Chinese)

Oliver S. C., Jamieson B. G. M., Scheltinga D. M. 1996. The ultrastructure of spermatozoa of Squamata, II, Agamidae, Varanidae, Colubridae, Elapidae, and Boidae (Reptilia). Herpetologica, 52: 216–241

Phillips D. M., Asa C. S. 1993. Strategies for formation of the midpiece. In Baccetti B. (Ed.), Comparative Spemiauilogy 20 Years After Serono Symp. New York: Raven Press, 75

Rheubert J. L., Siegel D. S., Venable K. J., Sever D. M., Gribbins K. M. 2011. Ultrastructural description of spermiogenesis within the Mediterranean Gecko, *Hemidactylus turcicus* (Squamata: Gekkonidae). Micron, 42: 680–690

Röll B., von Düring M. U. G. 2008. Sexual characteristics and spermatogenesis in males of the parthenogenetic gecko *Lepidoctylus lugubris* (Reptilia, Gekkonidae). Zoology, 5: 385–400

Scheltinga D. M., Jamieson B. G. M., Espinoza R. E., Orrell K. S. 2001. Descriptions of the mature spermatozoa of the lizards *Crotaphytus bicinctores*, *Gambelia wislizenii* (Crotaphytidae) and *Anolis carolinensis* (Polychrotidae) (Reptilia, Squamata, Iguania). J Morph, 247: 160–171

Teixeira R. D., Colli G. R., Báo S. N. 1999a. The ultrastructure of spermatozoa of the lizard *Polycbrus acutirostris* (Squamata, Polychrotidae). J Submicrosc Cytol Pathol, 31 : 387–395

Teixeira R. D., Colli G. R., Báo S. N. 1999b. The ultrastructure of the spermatozoa of the lizard *Micrablepharus maximiliani* (Squamata, Gymnophthalmidae), with considerations on the use of sperm ultrastructure characters in phylogenetic reconstruction. Acta Zool, 80: 47–59

Teixeira R. D., Colli G. R., Báo S. N. 1999c. The ultrastructure of the spermatozoa of the worm lizard *Amphisbaena alba* (Squamata, Gymnophthalmidae), and the phylogenetic relationships of amphisbaenians. Can J Zool, 77: 1254–1264

Tavares-Bastos L., Colli G. R., Báo S. N. 2008. The evolution of sperm ultrastructure among Boidae (Serpentes). Zoomorphology, 127: 189–202

Teixeira R. D., Vieira G. H. C., Colli G. R., Báo S. N. 1999d. Ultrastructural study of spermatozoa of the neotropical lizards , *Tropidurus semitaeniatus* and *Tropidurus torquatus* (Squamata, Tropiduridae). Tissue Cell, 31: 308–317

Tourmente M., Cardozo G., Bertona M., Guidobaldi A., Giojalas L., Chiaraviglio M. 2006. The ultrastructure of the spermatozoa of *Boa constrictor occidentalis*, with considerations on its mating system and sperm competition theories. Acta Zool, 87: 25–32

Tourmente M., Giojalas L., Chiaraviglio M. 2008. Sperm ultrastructure of *Bothrops alternatus* and *Bothrops diporus* (Viperidae, Serpentes), and its possible relation to the reproductive features of the species. Zoomorphology, 127: 241–248

Teixeira R. D., Scheltinga D. M., Trauth S. E., Colli G. R., Báo S. N. 2002. A comparative ultrastructural study of spermatozoa of the teiid lizards *Cnemidophorus gularis gularis*, *Cnemidophorus ocellifer*, and *Kentropyx altamazonica* (Reptilia, Squamata, Teiidae). Tissue Cell, 34 (3): 135–142

Tavares-Bastos L., Teixeira R. D., Colli G. R., Báo S. N. 2002. Polymorphism in the sperm ultrastructure among four species of lizards in the genus *Tupinambis* (Squamata: Teiidae). Acta Zool, 83: 297–307

Vieira G. H. C., Colli G. R., Báo S. N. 2004. The ultrastructure of the spermatozoon of the lizard *Iguana iguana* (Reptilia, Squamata, Iguanidae) and the variability of sperm morphology among iguanian lizards. J Anat, 204 (6): 451–464

Vieira G. H. C., Colli G. R., Báo S. N. 2005. Phylogenetic relationships of corytophanid lizards (Iguania, Squamata, Reptilia) based on partitioned and total evidence analyses of sperm morphology, gross morphology, and DNA data. Zool Scr, 34: 605–625

Vieira G. H. C., Cunha L. D., Scheltinga D. M., Glaw F., Colli G. R., Báo S. N. 2007. Sperm ultrastructure of hoplocercid and oplurid lizards (Sauropsida, Squamata, Iguania) and the phylogeny of Iguania. J Zool Syst Evol Res, 45(3): 230–241

Zhang Y. P., Fang Z. X., Ji X. 2006. A comparison of the ultrastructure of spermatozoa of two species of skinks *Mabuya multifasciata* and *Sphenomorphus indicus*. Acta Zool Sin, 52(3): 591–602 (In Chinese)

Zhang Y. P., Hu J. R., Ji X. 2004. Ultrastructure of spermatozoa of the Chinese skink *Eumeces chinensis*. Acta Zool Sin, 50 (3): 431–441 (In Chinese)

Zhang Y. P., Ying X. P., Ji X. 2005. Ultrastructure of spermatozoon of the northern grass lizard (*Takydromus septentrionalis*) with comments on the variability of sperm morphology among lizard taxa. Zool Res, 26(5): 518–526 (In Chinese)

Zhao E. M., Zhao K. T., Zhou K. Y. 1999. Fauna Sinica: Reptilia, Vol. 2, Squamata: Lacertilia. Beijing: Science Press (In Chinese)